

CLINICAL STUDIES

Short-Term Mechanical Unloading With Left Ventricular Assist Devices After Acute Myocardial Infarction Conserves Calcium Cycling and Improves Heart Function

Xufeng Wei, MD, PhD,*† Tieluo Li, MD,* Brian Hagen, PhD,‡ Pei Zhang, PhD,* Pablo G. Sanchez, MD, PhD,* Katrina Williams, BS,* Shuying Li, MD,§ Giacomo Bianchi, MD,|| Ho Sung Son, MD, PhD,¶ Changfu Wu, PhD,* Christopher DeFilippi, MD§ Kai Xu, PhD,* William J. Lederer, MD,‡ Zhongjun J. Wu, PhD,* Bartley P. Griffith, MD*

Baltimore, Maryland; Massa, Italy; and Seoul, Korea

Objectives This study sought to demonstrate that short-term cardiac unloading with a left ventricular (LV) assist device (LVAD) after acute myocardial infarction (MI) can conserve calcium cycling and improve heart function.

Background Heart failure secondary to MI remains a major source of morbidity and mortality. Alterations in calcium cycling are linked to cardiac dysfunction in the failing heart.

Methods Adult Dorsett hybrid sheep underwent acute MI and were mechanically unloaded with an axial-flow LVAD (Impella 5.0) for 2 weeks ($n = 6$). Six sheep with MI only and 4 sham sheep were used as controls. All animals were followed for 12 weeks post-MI. Regional strains in the LV were measured by sonomicrometry. Major calcium-handling proteins (CHPs), including sarco-/endoplasmic reticulum calcium ATPase-2 α (SERCA-2 α), Na⁺-Ca²⁺ exchanger-1, and phospholamban, and Ca²⁺-ATPase activity were investigated. The electrophysiological calcium cycling in single isolated cardiomyocytes was measured with the patch-clamp technique. The related ultrastructures were studied with electron microscopy.

Results LVAD unloading alleviated LV dilation and improved global cardiac function and regional contractility compared with the MI group. The regional myocardial strain (stretch) was minimized during the unloading period and even attenuated compared with the MI group at 12 weeks. Impaired calcium cycling was evident in the adjacent noninfarcted zone in the MI group, whereas CHP expression was normalized and Ca²⁺-ATPase activity was preserved in the LVAD unloading group. The electrophysiological calcium cycling was also conserved, and the ultrastructural damage was ameliorated in the unloaded animals.

Conclusions Short-term LVAD unloading may conserve calcium cycling and improve heart function during the post-infarct period. (J Am Coll Cardiol Intv 2013;xx:xxx) © 2013 by the American College of Cardiology Foundation

From the *Department of Surgery, University of Maryland School of Medicine, Baltimore, Maryland; †Department of Cardiac Surgery, Xijing Hospital, Xi'an, P. R. China; ‡Department of Physiology, University of Maryland School of Medicine, Baltimore, Maryland; §Department of Medicine, University of Maryland School of Medicine, Baltimore, Maryland; ||Ospedale del Cuore "G. Pasquinucci"—Fondazione Toscana Gabriele Monasterio CNR, Massa, Italy; and the ¶Department of Thoracic & Cardiovascular Surgery, Korea University, Seoul, Korea. The project was funded by the National Institutes of Health/National Heart, Lung, and Blood Institute (grant R01HL 081106 to Dr. Griffith) and by the William G. McGowan Charitable Fund. The authors have reported that they have no relationships relevant to the contents of this paper to disclose.

Manuscript received September 27, 2012; revised manuscript received October 26, 2012, accepted December 7, 2012.

Ischemic heart disease is the single leading cause of death and disability worldwide (1). Although acute treatment after myocardium infarction (MI) decreases early stage mortality, heart failure following deleterious remodeling becomes the main cause of morbidity and mortality (2,3). Angiotensin-converting enzyme (ACE) inhibition and beta-blockade effectively limit infarct expansion and remodeling after MI. Unfortunately, approximately 40% of MI patients still develop heart failure independent of the treatment received (1,3). Therefore, new strategies to prevent heart failure and remodeling after MI are needed.

Left ventricular (LV) assist devices (LVADs) have garnered great interest recently (4,5). Following LVAD implantation for the purpose of “bridging to transplant,” it became evident that

Abbreviations and Acronyms

ACE = angiotensin-converting enzyme

CaT = Ca^{2+} transient

CHP = calcium handling protein

EF = ejection fraction

I_{Ca} = inward Ca^{2+} current

LV = left ventricle/ventricular

LVAD = left ventricular assist device

LVEDV = left ventricular end-diastolic volume

LVESV = left ventricular end-systolic volume

MI = myocardial infarction

NCX-1 = Na^+ - Ca^{2+} exchanger-1

PLB = phospholamban

SERCA-2 α = sarco/endoplasmic reticulum calcium ATPase-2 α

SR = sarcoplasmic reticulum

some patients exhibited a substantial recovery in ventricular function. The remodeling reversal of end-stage heart failure by an LVAD alone or together with drug therapy has become a promising treatment (5). However, recovery sufficient to permit device removal has been observed in only 5% to 24% of patients in most studies, with a relatively high incidence of heart failure recurrence (6,7). This low percentage of recovery may be due to LVAD implantation at a stage too late for end-stage heart recovery. Irreversible changes in the failing heart may preclude the reversal of remodeling with LVAD unloading. In this study, we investigated the protection of heart function and the prevention of cardiac remodeling after acute MI with early intervention by the placement of a minimally invasive axial-flow LVAD.

Proper calcium handling in myocytes is controlled largely by the sarco-/endoplasmic reticulum calcium ATPase-2 α (SERCA-2 α), Na^+ - Ca^{2+} exchanger-1 (NCX-1), and phospholamban (PLB) (8,9). The alterations in the expression and function of these calcium-handling proteins (CHPs) are associated with myocardial hypocontractility. We examined CHP expression and electrophysiological calcium cycling in isolated single myocytes. The related ultrastructures of the sarcoplasmic reticulum (SR) and T-tubules were also examined in the infarcted hearts.

Methods

Surgery. Sixteen adult Dorsett hybrid sheep (53.2 ± 0.9 kg) were used in this study. Twelve sheep were subject to an apical MI by permanent coronary artery ligation. Six of

them were randomly assigned to the MI + LVAD group and were implanted with a microaxial LVAD to unload the infarcted heart during the first 2 weeks and monitored for an additional 10 weeks. Six sheep with MI only (MI group) and 4 sham sheep (sham group) were used as controls. All the animals were monitored for 12 weeks post-MI.

A left lateral thoracotomy was performed under general anesthesia. Sixteen sonomicrometry crystals were implanted to monitor LV regional movement and deformation. The coronary artery branches feeding the heart apex were ligated at one-third length of the LV, resulting in an apical MI (Fig. 1). Between 2 and 3 h after the MI in the MI + LVAD group, the microaxial pump (Impella 5.0, ABIOMED, Danvers, Massachusetts) was placed retrograde into the LV via a graft anastomosed to the descending aorta (Figs. 2A and 2B). The pump speed was set between 20,000 and 24,000 rpm (P_2 to P_4) to achieve $\sim 50\%$ unloading of the total cardiac output. After 2 weeks, the pump was removed, and the animals were followed for an additional 10 weeks. In the sham group, the animals underwent only sonomicrometry crystals implantation without MI and LVAD implantation.

All the animals were treated in compliance with the “Guide for the Care and Use of Laboratory Animals” (National Institutes of Health publication 85-23, revised 1996). All surgical procedures and post-operative care were approved by the Institutional Animal Care and Use Committee of the University of Maryland at Baltimore.

Cardiac function and remodeling evaluation. Echocardiograms were collected with a Sonos 5500 machine (Philips Medical, Andover, Massachusetts). The initial myocardial infarct size and the final infarct size were measured in the 2-dimensional apical 2-chamber view and presented as the length of wall motion abnormality. The final infarct size was confirmed at necropsy and presented as a ratio of infarcted scar area to the LV free wall. The total cardiac output was measured using a flow probe encompassing the pulmonary artery with a flow meter (T401, Transonic Systems, Ithaca, New York).

Sonomicrometry. The sonomicrometry was used to record the regional movement and deformation of the LV after MI as previously described (10,11). The regional contractile strain was defined as the LV movement during an individual cardiac cycle and calculated by the following: $\epsilon_{\text{contractile}} = S_{ED} - S_{ES} / S_{ED} \times 100\%$, where S_{ED} , S_{ES} = the triangular area at end-diastolic and end-systolic instants, respectively. The regional diastolic strain (stretch) was defined as the LV deformation over time and was calculated by comparing the end-diastole geometries at 1 data collection time point to the pre-MI measurement by the following: $\epsilon_{\text{diastolic}} = S_{ED} - S_{ED\text{pre-MI}} / S_{ED\text{pre-MI}} \times 100\%$, where $S_{ED\text{pre-MI}}$ = the triangular area at end-diastolic instant pre-MI.

Western immunoblot analysis. Protein extraction, Western immunoblotting, and densitometry were performed as de-

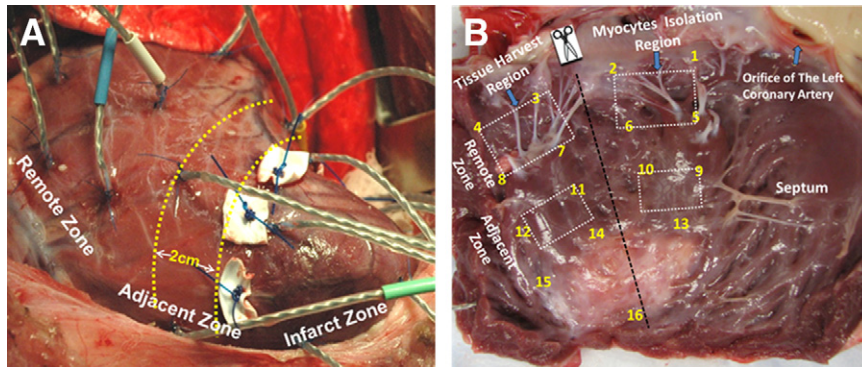


Figure 1. Myocardial Infarction and the Division of the Infarcted Heart

(A) An infarcted heart with 16 sonomicrometry crystals on the left ventricular free wall. The adjacent zone was defined as the border zone within 2 cm of the infarct zone. (B) Tissue harvesting at autopsy.

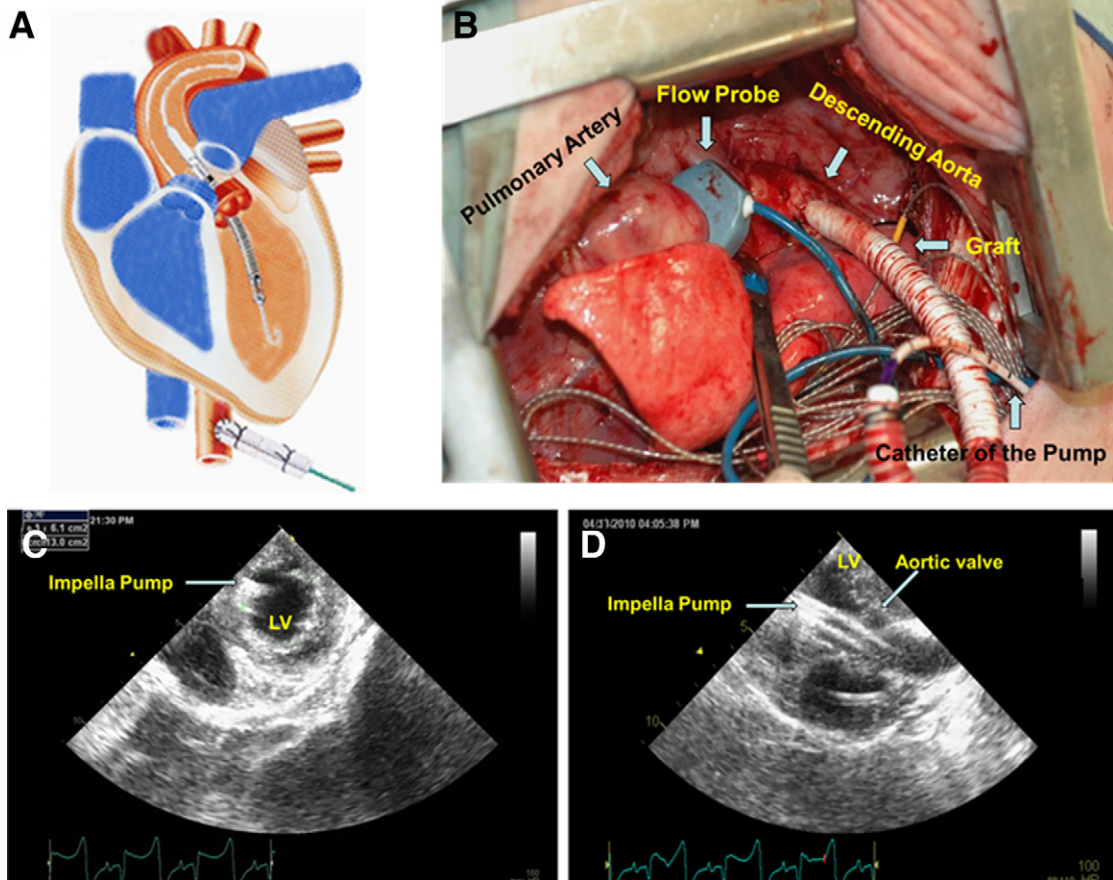
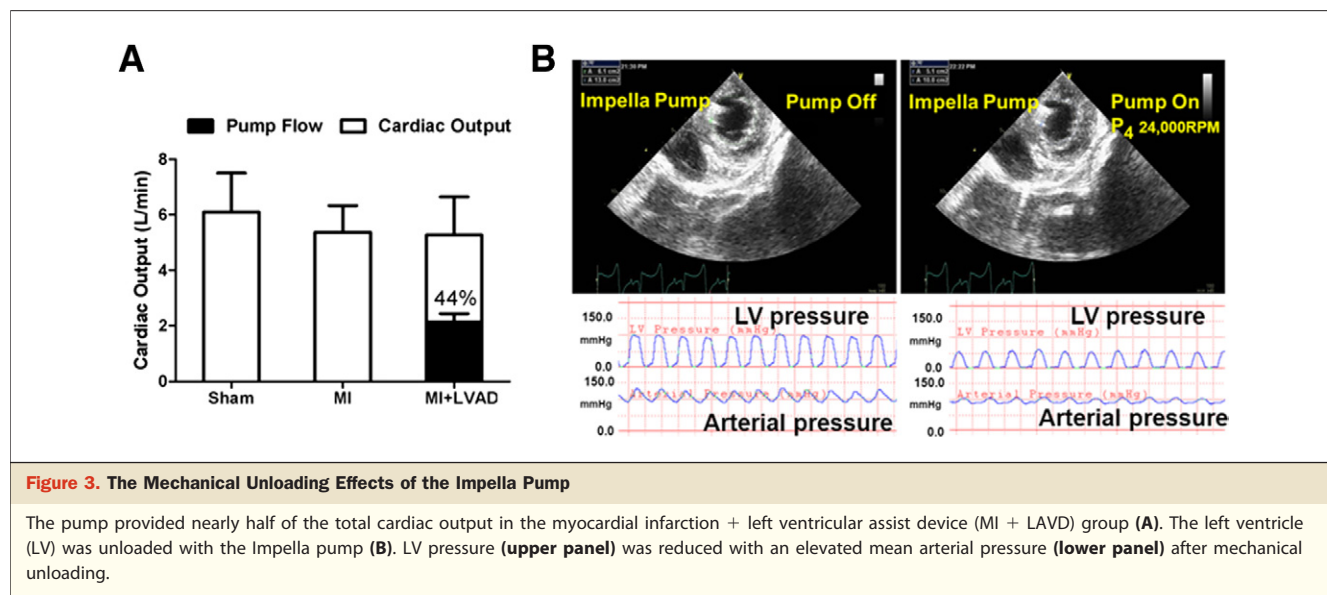


Figure 2. Implantation of the Impella Pump

A microaxial pump was implanted retrograde into the left ventricle (LV) via the graft, descending aorta, and the aortic valve (A and B). Positioning of the device was monitored by echocardiography (C and D).



scribed previously (10,12). Primary antibodies included anti-SERCA-2 α (110 kDa) (Novocastra, Newcastle, United Kingdom), anti-NCX-1 (75 kDa) (Abcam, Cambridge, Massachusetts), and anti-PLB (25 and 5 kDa) (Affinity BioReagents, Golden, Colorado). GAPDH (glyceraldehyde-3-phosphate dehydrogenase) (Santa Cruz Biotechnology, Santa Cruz, California) was used as an internal control. The results are expressed as the ratio of the target protein to GAPDH.

Determination of SR Ca²⁺-ATPase activity. The ATPase assay was a modification of the method described by Kyte (13). Enzymatic activity was defined as the thapsigargin (Tg)-sensitive hydrolysis of MgATP in the presence of 10 μ M Ca²⁺.

Cardiomyocyte isolation. Single ventricular myocytes were isolated from the LV wall by enzymatic dissociation modified from Zafeiris et al. (14) on the human heart. Briefly, collagenase was perfused from the left coronary artery followed by a wash solution containing taurine (Fig. 1B). Myocytes from the adjacent and remote zones were separated by mechanical agitation and were reintroduced to 1.8 mM Ca²⁺ in a stepwise fashion.

Electrophysiological Ca²⁺ cycling. The electrophysiological Ca²⁺ cycling was measured as previously described (15). In brief, patch clamps were used to control membrane voltage and measure membrane current while simultaneously imaging [Ca²⁺]_i was performed using laser scanning confocal microscopy with the Ca²⁺ indicator fluo-4 (Molecular Probes, Eugene, Oregon). Inward current recording was performed in Tyrode solution in which K⁺ was replaced by Cs⁺. Ca²⁺ currents were recorded at a membrane potential between -50 and 40 mV (10-mV steps), and Na⁺ channels were inactivated by an increase from -80 to -50 mV over 500 ms. The cellular [Ca²⁺]_i transient (CaT) was measured

by the fluo-4 signal using rapid line-scan imaging. The L-type Ca²⁺ channel current (I_{Ca}) was measured directly.

Electron microscopy. Processed tissues were examined using a FEI Tecnai T12 electron microscope (FEI, Hillsboro, Oregon). A heart injury scoring system for the quantitative evaluation of the SR ultrastructural findings in every field was used as previously described (16). Normal SR ultrastructure was scored as 0. Mildly dilated tissue was scored as 1, the presence of vacuoles was scored as 2, and largely degenerated areas were scored as 3.

Statistics. All data are presented as the mean \pm SEM. Two-way repeated measures analysis of variance was used to compare differences among the groups. All analyses of variance were followed by multiple comparisons with the Bonferroni correction. A comparison of protein expression in a same sheep (the adjacent zone vs. the remote zone) was performed with a Student paired *t* test. Probability values <0.05 were considered statistically significant.

Results

Unloading effects of the LVAD. In the MI + LVAD group, the average pump flow was 2.14 \pm 0.30 l/min during the first 2 weeks. The LVAD unloaded 43.6 \pm 13.2% of the total cardiac output in the LV (Fig. 3A). Echocardiography showed that the short-axial area of the LV decreased under unloading with the LVAD. LV pressure was reduced significantly with LVAD unloading (Fig. 3B).

Cardiac remodeling and function evaluated by echocardiography. LVAD unloading prevented cardiac remodeling and dysfunction after MI. There was no difference in the baseline LV end-diastolic volume (LVEDV), end-systolic volume (LVESV), and LV ejection fraction (LVEF) among the groups (pre-MI and post-MI). In the MI group, the

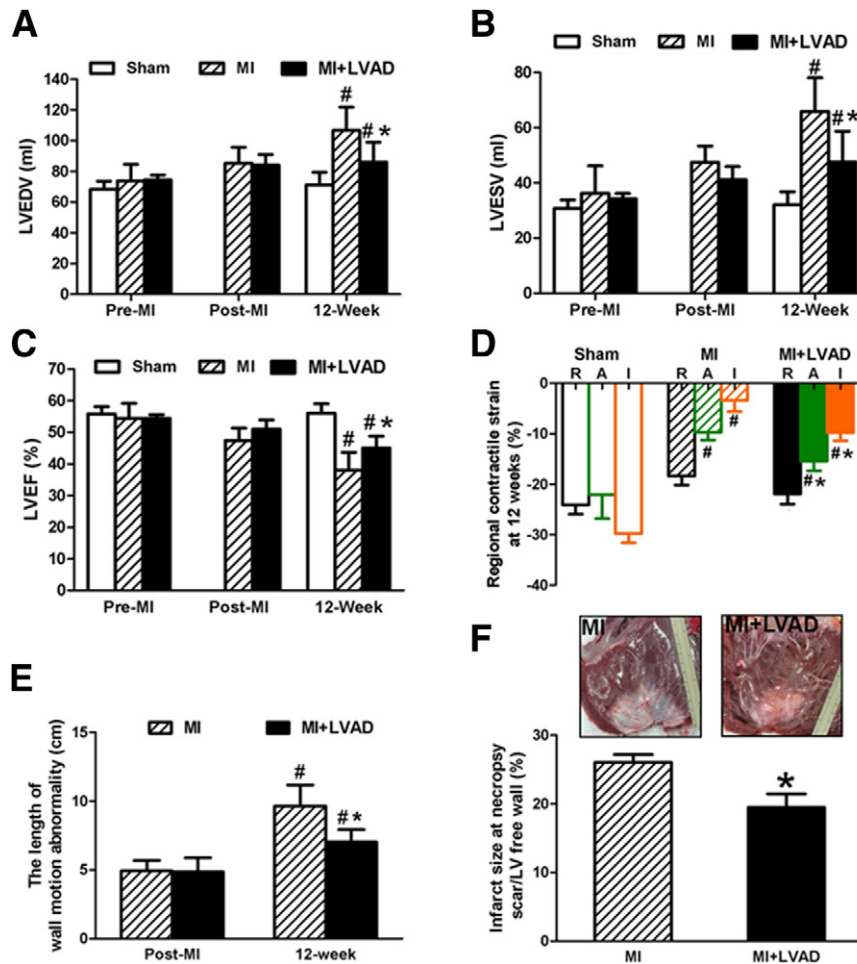


Figure 4. Cardiac Function and Remodeling After MI and Unloaded by LVAD

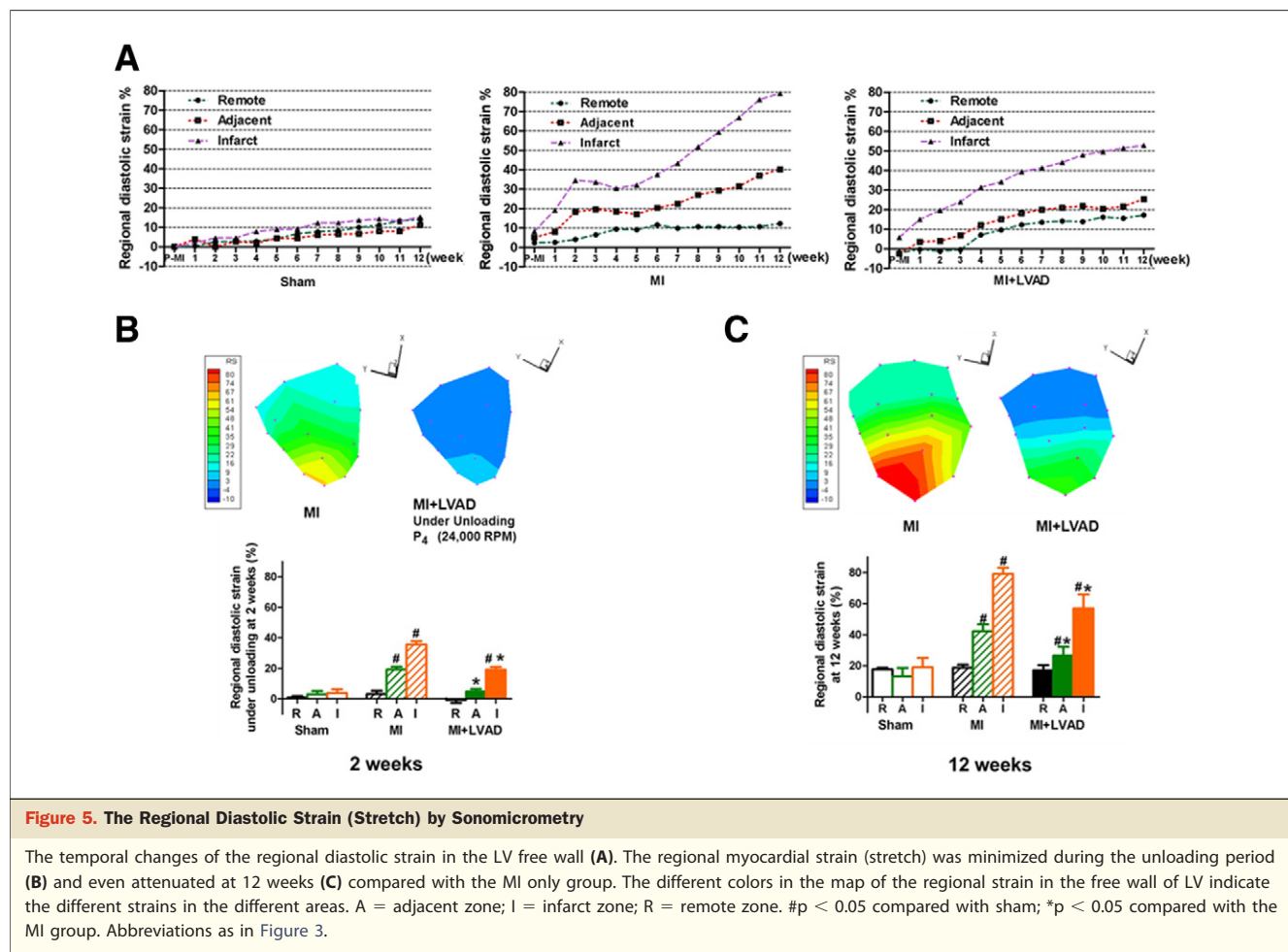
Dilation of LV was prevented in the unloaded group, which was indicated by the LV end-diastolic volume (LVEDV) (A) and LV end-systolic volume (LVESV) (B). The LV ejection fraction (LVEF) value decreased less in the MI + LVAD group compared with the MI group at 12 weeks (C). Regional contractile strain at 12 week calculated by sonomicrometry showed that the myocardial contractility in the adjacent zone was conserved in the MI + LVAD group and remained almost normal in the remote zone (D). The length of wall motion abnormality evaluated by echocardiography (E) and infarct size at necropsy (F) showed that the MI + LVAD group had significantly smaller infarct size than the MI group. # $p < 0.05$ compared with the baseline; * $p < 0.05$ compared with the MI group. Abbreviations as in Figure 3.

LVEDV and LVESV increased over 12 weeks ($p < 0.05$). In the MI + LVAD group, the LVEDV and LVESV increased at 12 weeks but to a significantly lesser extent compared with the MI group (Figs. 4A and 4B) (LVEDV: 85.9 ± 6.2 ml vs. 106.6 ± 5.9 ml; LVESV: 47.6 ± 5.0 ml vs. 65.9 ± 4.9 ml, $p < 0.05$). In the MI group, the LVEF decreased over 12 weeks. Whereas in the MI + LVAD group, LVAD unloading improved the LVEF compared with the MI group (Fig. 4C) ($45 \pm 1.7\%$ vs. $38.1 \pm 2.4\%$, $p < 0.05$).

Regional contractility by sonomicrometry. In the MI group, the regional contractile strain was decreased in the noninfarcted adjacent zone and remote zone at 12 weeks compared with the sham group (Fig. 4D). By contrast, In the

MI + LVAD group, the regional systolic strain in the adjacent zone was significantly greater compared with the MI group ($-15.4 \pm 1.9\%$ vs. $-9.7 \pm 1.5\%$, $p < 0.05$), and the remote zone had nearly normal contractility compared with the sham group at 12 weeks.

LVAD unloading reduced the infarct size. The length of wall motion abnormality at 30 min post-MI had no statistical difference in the MI group and the MI + LVAD group. However, the length of wall motion abnormality at the time of sacrifice was shorter in the MI + LVAD group than in the MI group (Fig. 4E). Infarct size measured at necropsy confirmed that LVAD unloading led to a significant decrease of infarct size ($26.4 \pm 1.5\%$ vs. $19.5 \pm 2.0\%$, $p < 0.05$) (Fig. 4F).



Regional diastolic strain (stretch) by sonomicrometry. The temporal changes of the diastolic strain in the infarcted zone, adjacent zone, and remote zone in the LV free wall are shown in Figure 5A. The further comparison of the diastolic strain during mechanical unloading (at 2 weeks) and 10 weeks after removal of the pump (at 12 weeks) are shown in Figures 5B and 5C, respectively. After MI, the regional myocardial strain increased heterogeneously. In the MI group, the diastolic strain in the infarcted zone and in the adjacent zone increased quickly in the first 2 weeks and continuously increased in 12 weeks. By contrast, in the MI + LVAD group, the diastolic strain in the remote zone, adjacent zone, and even for the infarcted zone was low under the LVAD unloading (Fig. 5B). Ten weeks after removal of the pump in the MI + LVAD group, the diastolic strain increased but was significantly lower in the adjacent and infarct zones compared with the MI group ($26.7 \pm 5.6\%$ vs. $42.3 \pm 4.4\%$; $57.0 \pm 9.0\%$ vs. $79.1 \pm 4.0\%$, respectively, $p < 0.05$) (Fig. 5C).

CHP expression. In the MI group, SERCA-2 α expression decreased significantly in the adjacent zone compared with the remote zone or the sham group (Fig. 6A) (1.49 ± 0.12

vs. 1.97 ± 0.12 or 1.96 ± 0.08 , respectively, $p < 0.05$). NCX-1 expression was increased both in the adjacent and remote zones compared with the sham group. The adjacent zone had even higher NCX-1 expression compared with the remote zone (Fig. 6B). PLB (5 kDa) remained unchanged both in the remote and the adjacent zones. The PLB pentamer (25 kDa), as the reservoir form of PLB, was decreased in the adjacent zone compared with the sham group (Fig. 6C) (1.65 ± 0.27 vs. 2.82 ± 0.17 , $p < 0.05$). In the MI + LVAD group, CHP expression remained essentially normal compared with the sham group, and there was no significant difference between the adjacent zone and the remote zone.

Ca²⁺-ATPase activity. In the MI group, Ca²⁺-ATPase activity was significantly reduced by $53 \pm 4\%$ in the adjacent zone compared with the sham group (Fig. 6D). By contrast, in the MI + LVAD group, the Ca²⁺-ATPase activity in the adjacent zone remained unchanged and was significantly higher compared with the MI group ($105 \pm 10\%$ vs. $53 \pm 4\%$, $p < 0.05$).

Calcium cycling in isolated single cardiomyocytes. Sample data of the Ca²⁺ imaging, the CaT, and I_{Ca} are presented in Figure 7A. The average I_{Ca} peak and CaT amplitude in

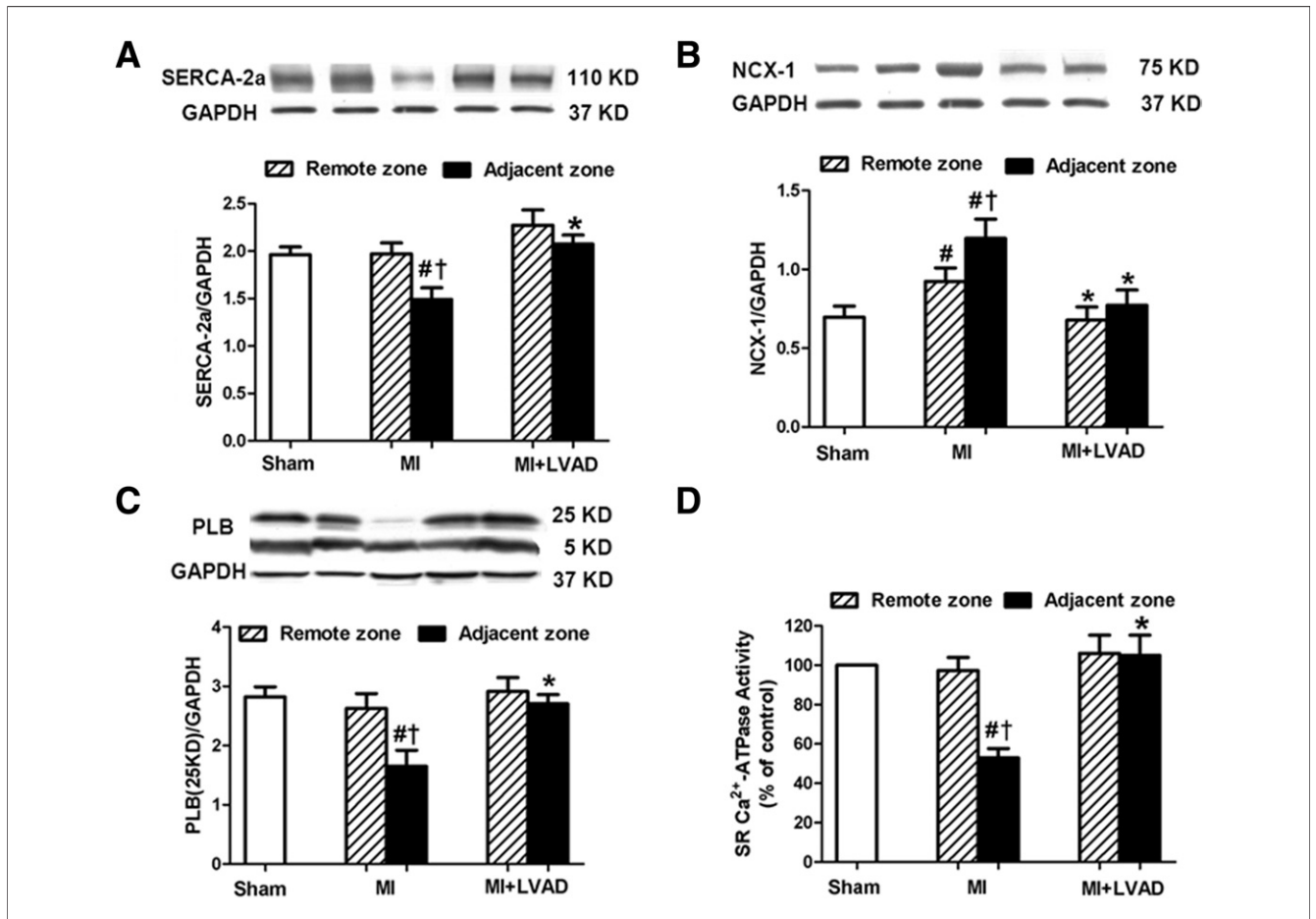


Figure 6. CHP Expression and Ca²⁺-ATPase Activity

Alterations in SERCA-2 α (A), NCX-1 (B), and the PLB pentamer (C) were normalized in the MI + LVAD group. LVAD unloading prevented post-MI impairment of SR Ca²⁺-ATPase activity in the adjacent zone (D). #p < 0.05 compared with sham; *p < 0.05 compared with the MI group; †p < 0.05 compared with the remote zone of same animal. SR = sarcoplasmic reticulum; other abbreviations as in Figure 3.

the myocytes isolated from the remote zone in the MI or MI + LVAD group was not different compared with the myocytes in the sham group. In the MI group, the myocytes from the adjacent zone showed a significant decrease in the I_{Ca} peak and CaT compared with the remote zone -1.63 ± 0.09 versus -2.51 ± 0.22 ($p < 0.05$) and 2.53 ± 0.21 versus 3.08 ± 0.14 ($p < 0.05$), respectively. In the MI + LVAD group, the myocytes had no significant difference in I_{Ca} or CaT between the adjacent and remote zones (Figs. 7B and 7C). The time required for the CaT to reach its peak (rise time) was also significantly slower in the myocytes from the adjacent zone of the MI group. This was not observed in the myocytes isolated from the MI + LVAD group (Fig. 7D). In the MI group, the recovery rate for the Ca²⁺ transient (decay time) in the myocytes from the adjacent zone was significantly slower than in the myocytes from the remote zone (1.02 ± 0.04 vs. 0.78 ± 0.06 , $p < 0.05$). Again, this trend was not observed in the MI + LVAD group (Fig. 7E).

LVAD unloading protected against ultrastructural damage

after MI. Myocardial ultrastructural damage was found in the adjacent zone of the MI group. Damaged SR was swollen or missing membrane structures. The structure of the T-tubules became unclear, and its arrangement became irregular (Figs. 8B and 8E). In the MI + LVAD group, most SR had a normal ultrastructure (Fig. 8C) and a regular arrangement of T-tubules (Fig. 8F), similar to the sham group (Figs. 8A and 8D). Injury scoring of the SR revealed that unloading with the LVAD led to a significant decrease in SR damage in the adjacent zone compared with the MI group (Fig. 8G).

Discussion

Currently, LVADs have 3 main applications in end-stage heart failure: “bridge to transplantation,” “bridge to recovery,” and destination therapy (4,17). LVADs have also been used for short-term circulatory support in patients with cardiogenic shock when traditional inotropic medications

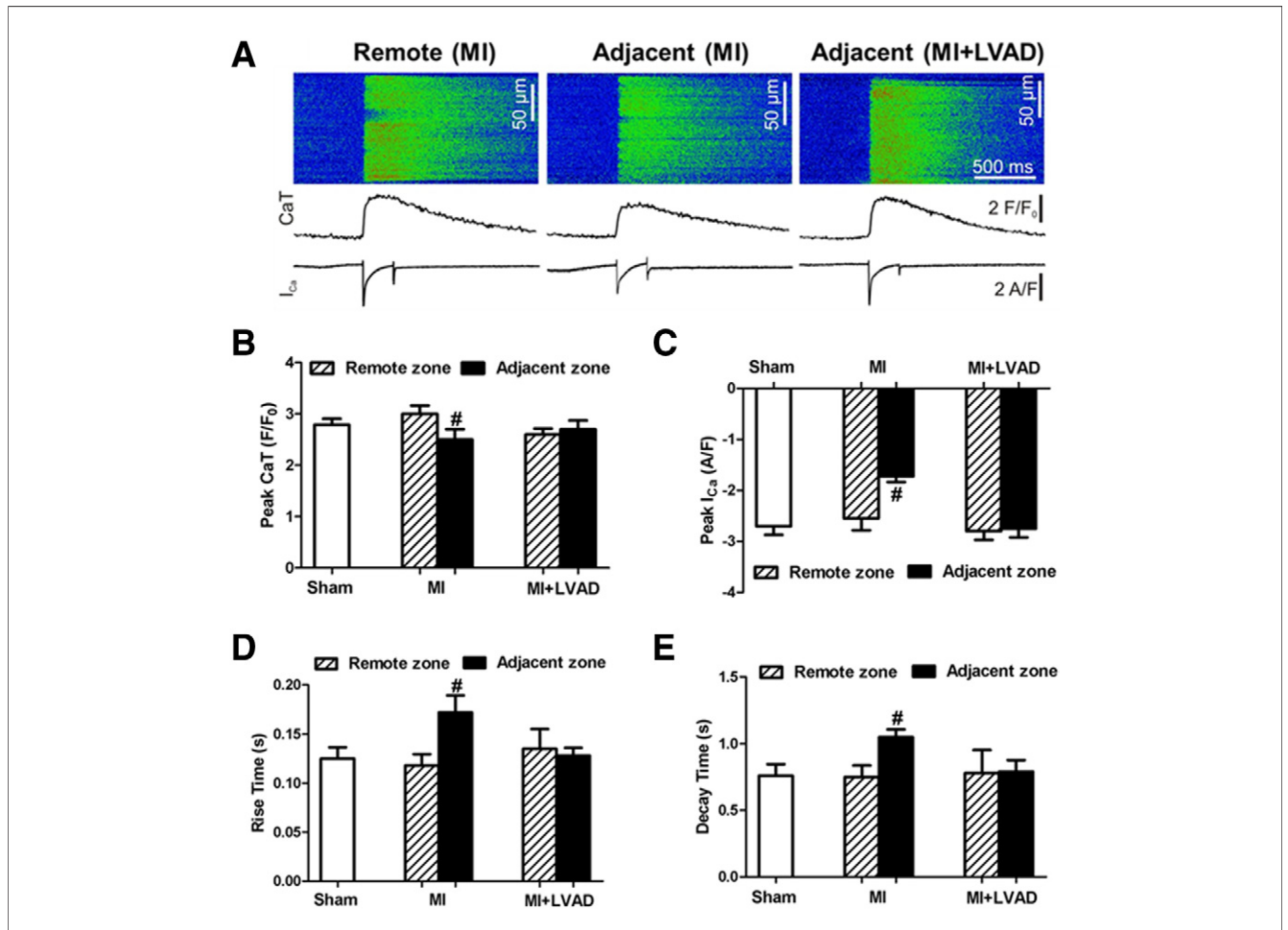


Figure 7. Electrophysiological Ca²⁺ Cycling in Single Cardiomyocytes

(A) Fluorescence of the Ca²⁺ indicator fluo-4 (top panels and middle traces) and whole-cell membrane currents during a voltage increase from -80 to 0 mV after inactivating the Na⁺ channels (bottom traces). (B) The average peak Ca²⁺ transient (CaT). (C) The peak inward Ca²⁺ current (peak I_{Ca}). (D) The time the Ca²⁺ transients took to reach the peak (rise time). (E) The time required for the transients to decay from 90% of the peak to 10% (decay time). #p < 0.05 compared with the remote zone of same animal. Abbreviations as in Figure 3.

and temporary circulatory support with an intra-aortic balloon pump have failed. The safety and efficacy of LVAD support were well demonstrated from these short-term follow-up data (18,19). In this study, a minimally invasive axial-flow pump was used, not for circulatory support, but for LV unloading to prevent post-MI remodeling and chronic heart failure, which makes this study the first of its kind to our knowledge.

Two major explanations exist for the beneficial effects of an LVAD upon cardiac performance even in the short term. First, the increased mechanical stress on the noninfarcted myocardium after MI causes multiple downstream molecular changes, which promote heart failure development (2,20,21). Cardiac dysfunction further increases the mechanical strain/stress in a vicious cycle. A strain reduction by unloading with LVAD can disrupt the vicious cycle and inhibit harmful molecular events, including deleterious

Ca²⁺ cycling, and prevent progression of negative remodeling after MI (9,22,23). Second, our study determined that the regional strain increased dramatically in the first 2 weeks (Fig. 5A), suggesting that this time period is crucial regarding myocardium damage and the subsequent development of heart failure. LVADs can provide profound circulatory support in addition to mechanical LV unloading in this phase, which makes it unique for MI therapy.

Ca²⁺ cycling, a key mechanism for generating contractile force, has been linked to myocardial contractile dysfunction in heart failure. Most reports have indicated that SERCA-2 α levels are decreased, and NCX-1 is up-regulated, whereas the levels of PLB remain unchanged in the end-stage failing heart (8,24). Yoshiyama et al. (25) reported regional differences in the expression of SERCA-2 α and NCX-1 at the mRNA level after MI in a rat animal model. SERCA-2 α mRNA levels in the adjacent myo-

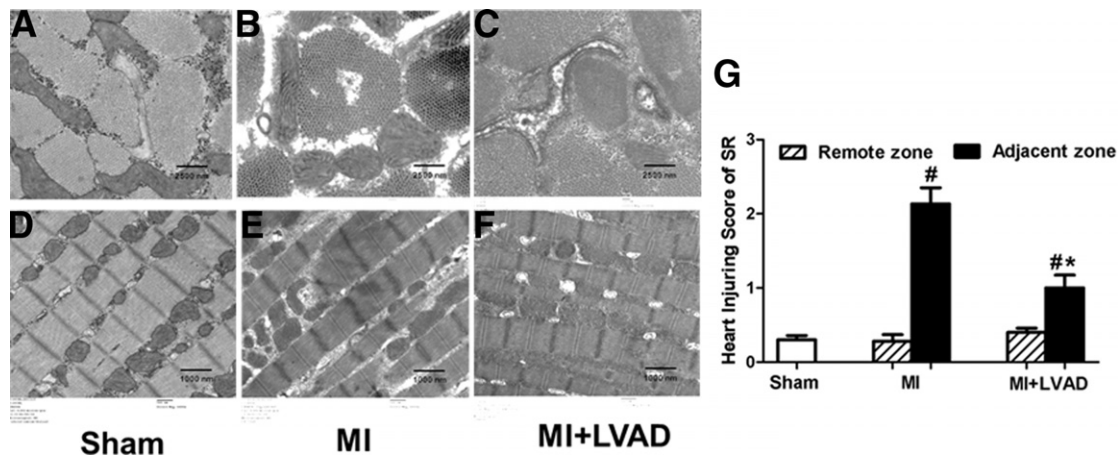


Figure 8. Ultrastructural Damage

(A, B, and C) Cross-section (11,000 \times). (D, E, and F) Longitudinal section (4,400 \times). (G) Heart injury scoring for the SR. # $p < 0.05$ compared with sham; * $p < 0.05$ compared with the MI group. Abbreviations as in Figure 3.

cardium decreased, whereas NCX-1 mRNA levels were increased 3 months after infarction. Consistent results were found at the protein level in this study. We further demonstrated that the changes in expression in SERCA-2 α and NCX-1 are heterogeneous after MI. Calcium handling in isolated single cardiac myocytes and ultrastructural damage were also present in the adjacent zone. These alterations in calcium handling provide an explanation for the hypocontractility observed in the perfused, nonischemic adjacent zone and a mechanism for remodeling after MI.

Calcium cycling is a mechanosensitive event (26). Previously, we also reported that the regional alteration on calcium handling proteins are strain (stretch) related during remodeling post-MI (12). In the present study, we further demonstrated that mechanical unloading with an LVAD reduced regional strain and normalized calcium cycling. These data from the large animal model support that the close relation between calcium cycling and the mechanical signal. However, it was reported that decreased abundance of mRNA of SERCA-2 α in heart failure could not be normalized by LVAD support in the end-stage heart failure patients (9,27). These findings strongly supported the advantages of the “prevention of remodeling” over “reversal of remodeling.”

Study limitations. Neither group received the current standard of care for post-MI patients, such as ACE inhibition and beta-blockade, in the present study. Because the overall goal of this study to evaluate the effects of stress reduction on the ventricular wall by mechanical unloading, we decided not to include at this time a group with a combined therapy (ACEI-beta-blockers plus LVADs). We are currently planning this set of experiments.

Conclusions

Short-term unloading with LVADs after acute MI normalized CHP alterations, conserved electrophysiological calcium cycling, and precluded damage of the calcium handling-related ultrastructures to improve myocardial contractility and prevent remodeling after MI.

Reprint requests and correspondence: Dr. Zhongjun J. Wu or Dr. Bartley P. Griffith, Department of Surgery, University of Maryland School of Medicine, MSTF Building 436 and 10 South Pine Street, Baltimore, Maryland 21201, E-mail: zwu@smail.umaryland.edu or bgriffith@smail.umaryland.edu.

REFERENCES

- Lloyd-Jones DM, Hong Y, Labarthe D, et al. Defining and setting national goals for cardiovascular health promotion and disease reduction: the American Heart Association's strategic Impact Goal through 2020 and beyond. *Circulation* 2010;121:586–613.
- Cohn JN, Ferrari R, Sharpe N, on behalf of an International Forum on Cardiac Remodeling. Cardiac remodeling—concepts and clinical implications: a consensus paper from an international forum on cardiac remodeling. *J Am Coll Cardiol* 2000;35:569–82.
- French BA, Kramer CM. Mechanisms of post-infarct left ventricular remodeling. *Drug Discov Today Dis Mech* 2007;4:185–96.
- Rose EA, Gelijns AC, Moskowitz AJ, et al. Long-term use of a left ventricular assist device for end-stage heart failure. *N Engl J Med* 2001;345:1435–43.
- Birks EJ, Tansley PD, Hardy J, et al. Left ventricular assist device and drug therapy for the reversal of heart failure. *N Engl J Med* 2006;355:1873–84.
- Mancini DM, Beniaminovit A, Levin H, et al. Low incidence of myocardial recovery after left ventricular assist device implantation in patients with chronic heart failure. *Circulation* 1998;98:2383–9.
- Maybaum S, Mancini D, Xydas S, et al. Cardiac improvement during mechanical circulatory support: a prospective multicenter study of the LVAD Working Group. *Circulation* 2007;115:2497–505.

8. Lompré AM, Hajjar RJ, Harding SE, Kranias EG, Lohse MJ, Marks AR. Ca^{2+} cycling and new therapeutic approaches for heart failure. *Circulation* 2010;121:822–30.
9. Chaudhary KW, Rossman EI, Piacentino V III, et al. Altered myocardial Ca^{2+} cycling after left ventricular assist device support in the failing human heart. *J Am Coll Cardiol* 2004;44:837–45.
10. Li T, Kilic A, Wei X, et al. Regional imbalanced activation of the calcineurin/BAD apoptotic pathway and the PI3K/Akt survival pathway after myocardial infarction. *Int J Cardiol* 2011 Nov 14 [E-pub ahead of print].
11. Yankey GK, Li T, Kilic A, et al. Regional remodeling strain and its association with myocardial apoptosis after myocardial infarction in an ovine model. *J Thorac Cardiovasc Surg* 2008;135:991–8.
12. Kilic A, Li T, Nolan TD, et al. Strain-related regional alterations of calcium-handling proteins in myocardial remodeling. *J Thorac Cardiovasc Surg* 2006;132:900–8.
13. Kyte J. Purification of the sodium- and potassium-dependent adenosine triphosphatase from canine renal medulla. *J Biol Chem* 1971;246:4157–65.
14. Zafeiridis A, Jeevanandam V, Houser SR, Margulies KB. Regression of cellular hypertrophy after left ventricular assist device support. *Circulation* 1998;98:656–62.
15. Cannell MB, Berlin JR, Lederer WJ. Effect of membrane potential changes on the calcium transient in single rat cardiac muscle cells. *Science* 1987;238:1419–23.
16. Ozisik K, Yildirim E, Kaplan S, Solaroglu I, Sargon MF, Kilinc K. Ultrastructural changes of rat cardiac myocytes in a time-dependent manner after traumatic brain injury. *Am J Transplant* 2004;4:900–4.
17. Lietz K, Long JW, Kfoury AG, et al. Outcomes of left ventricular assist device implantation as destination therapy in the post-REMATCH era: implications for patient selection. *Circulation* 2007;116:497–505.
18. Seyfarth M, Sibbing D, Bauer I, et al. A randomized clinical trial to evaluate the safety and efficacy of a percutaneous left ventricular assist device versus intra-aortic balloon pumping for treatment of cardiogenic shock caused by myocardial infarction. *J Am Coll Cardiol* 2008;52:1584–8.
19. Sjauw KD, Konorza T, Erbel R, et al. Supported high-risk percutaneous coronary intervention with the Impella 2.5 device: the Europella registry. *J Am Coll Cardiol* 2009;54:2430–4.
20. Mann DL, Bristow MR. Mechanisms and models in heart failure: the biomechanical model and beyond. *Circulation* 2005;111:2837–49.
21. Jackson BM, Gorman JH, Moainin SL, et al. Extension of borderzone myocardium in postinfarction dilated cardiomyopathy. *J Am Coll Cardiol* 2002;40:1160–7.
22. Hall JL, Fermin DR, Birks EJ, et al. Clinical, molecular, and genomic changes in response to a left ventricular assist device. *J Am Coll Cardiol* 2011;57:641–52.
23. Klotz S, Barbone A, Reiken S, et al. Left ventricular assist device support normalizes left and right ventricular beta-adrenergic pathway properties. *J Am Coll Cardiol* 2005;45:668–76.
24. MacLennan DH, Kranias EG. Phospholamban: a crucial regulator of cardiac contractility. *Nat Rev Mol Cell Biol* 2003;4:566–77.
25. Yoshiyama M, Takeuchi K, Hanatani A, et al. Differences in expression of sarcoplasmic reticulum Ca^{2+} -ATPase and Na^{+} - Ca^{2+} exchanger genes between adjacent and remote noninfarcted myocardium after myocardial infarction. *J Mol Cell Cardiol* 1997;29:255–64.
26. Lammerding J, Kamm RD, Lee RT. Mechanotransduction in cardiac myocytes. *Ann N Y Acad Sci* 2004;1015:53–70.
27. Bartling B, Milting H, Schumann H, et al. Myocardial gene expression of regulators of myocyte apoptosis and myocyte calcium homeostasis during hemodynamic unloading by ventricular assist devices in patients with end-stage heart failure. *Circulation* 1999;100:II216–23.

Key Words: calcium cycling ■ cardiac remodeling ■ heart failure ■ left ventricular assist devices ■ myocardial infarction.